Polyelectrolyte Layer by Layer Assembly on Organic Electrochemical Transistors

Anna-Maria Pappa[1#], Sahika Inal [1,2#], Kirsty Roy[1], Yi Zhang[1], Charalampos Pitsalidis[1], Adel Hama[1], Jolien Pas[1], George G. Malliaras[1] and Roisin M. Owens[1]**

[1] Department of Bioelectronics, Ecole Nationale Supérieure des Mines, CMP-EMSE, MOC, 13541 Gardanne, France

[2] Biological and Environmental Science and Engineering, King Abdullah University of Science and Technology (KAUST), Thuwal, 23955-6900, Kingdom of Saudi Arabia

Corresponding Authors: owens@emse.fr; sahika.inal@kaust.edu.sa.

# these authors contributed equally to this work

KEYWORDS: Layer-by-Layer, Organic transistor, Conducting polymer, Polyelectrolyte, Nucleic acid

ABSTRACT

Oppositely charged polyelectrolyte multilayers (PEMs) were built-up in a layer-by-layer (LbL) assembly on top of the conducting polymer channel of an organic electrochemical transistor (OECT), aiming to combine the advantages of well-established PEMs with a high performance electronic transducer. The multilayered film is a model system to investigate the impact of biofunctionalization on the operation of OECTs comprising a poly(3,4-ethylenedioxythiophene) polystyrene sulfonate (PEDOT:PSS) film as the electrically active layer. Understanding the mechanism of ion injection into the channel that is in direct contact with charged polymer films provides useful insights for novel biosensing applications such as nucleic acid sensing. Moreover, LbL is demonstrated to be a versatile electrode modification tool enabling tailored surface features in terms of thickness, softness, roughness, and charge. LbL assemblies built-up on top of conducting polymers will aid the design of new bioelectronic platforms for drug-delivery, tissue engineering and medical diagnostics.

INTRODUCTION

The discovery of conducting polymers (CPs) has fueled research in multiple areas, and recently in the field of bioelectronics, coupling conventional electronics with biology.[1,2] The ability of CPs to conduct both electrons and ions, in combination with their soft nature and compatibility with biological species, are only some of the merits that render these materials a promising conduit between electronics and biology.[3] The field of organic bioelectronics leverages the properties of CPs to improve the biotic/abiotic interface, aiming to address unmet clinical needs.[4] For organic bioelectronic devices, the interface of the CP (the abiotic electronic component) with the biological milieu is of utmost importance, dictating most chemical, biological or electrical processes.[5] The ability to control and tailor this interface, either through post-processing or via synthesis, can endow devices with new functionalities, e.g. detection or stimulation of a biological process, which may otherwise be infeasible or inefficient with unmodified CP electrodes.[6] Synthetic routes are generally tedious, with the disadvantage of possibly interfering with the overall device performance, considering that electrical properties of CPs are often reported to be very sensitive to changes in the chemical structure.[7] Another point to take into account is that adsorption of a bio-active compound onto a solid substrate can introduce conformational changes in the molecule which may reduce, if not eliminate bioactivity.[8]

Layer-by-layer (LbL) assembly, first established by Decher et al,[9] is a bottom-up nanofabrication technique for multilayer formation on top of a desired substrate.[10] LbL assembly can generally be built up by alternating deposition of mutually interacting species such as oppositely charged polyelectrolytes, yielding polyelectrolyte multilayers (PEMs) that represent the majority of the LbL generated films studied to date.[11] Other PEM deposition techniques have

been reported to be less versatile than LbL mostly due to limited type of assembly components (Langmuir-Blodgett type deposition is limited to amphiphilic molecules) and the requirement of certain chemical species on the surface for the attachment of the layers (e.g. self-assembled monolayers).[10] Given that most bioactive compounds have charged sites at their surfaces, LbL can also be applied to construct architectures including biological molecules.[10] The variety of materials that can be deposited as thin films using this technique, the mild processing conditions compatible with physiological conditions and its cost-effectiveness, as well as the control and tunability of the film properties, render LbL ideal for functionalizing surfaces with biological compounds.[12,13] Moreover, the use of the LbL technique for deposition/encapsulation of electroactive materials has enabled electro-responsive films that are promising for biology-related applications.[14] For instance, electrical stimulation of LbL films comprising electroactive components has been reported to induce local changes in pH, ionic strength or even water electrolysis. These led to destabilization of the films and thus the release of the incorporated bio-active molecules such as DNA[15] or drugs.[16,17] Another work reported an LbL assembly of a redox active polymer and DNA that could electrochemically detect the oxidative damage of DNA.[18] Introduction of a redox enzyme such as lactate oxidase within an LbL assembly, at the gate of a field effect transistor resulted in sensitive detection of the corresponding metabolite, lactate, due to the preservation of the enzymatic activity.[19] Organic electrochemical transistors (OECTs) can efficiently transduce, as well as amplify, small ionic fluxes in biological systems into electrical outputs. The channel of the transistor, comprised typically of the CP PEDOT:PSS, is gated through an electrolyte (the biological medium), and any changes at this interface are expected to change the current outputs. OECTs differ from other electrolyte gated transistors in that the change in electronic charge density occurs over the entire volume of the channel,

providing efficient ionic-to-electronic current transduction and leading to a high transconductance. [20] The transconductance (so far the highest reported among electrolyte-gated counterparts)[21] translates into high sensitivity in biosensing applications. OECTs have therefore been used for sensing of various biological species ranging from ions[22] to metabolites,[23,24] and processes such as cell proliferation and differentiation.[25,26]

In this work, we introduce for the first time, an LbL assembly of alternating polyelectrolytes, namely poly-L-lysine (PLL) and polystyrene sulfonate (PSS), on top of the channel of a PEDOT:PSS based OECT combining the advantages of well-established PEMs as a sensitive biofunctionalization approach with a highly performant electronic device. We demonstrate the formation of LbLs on the PEDOT:PSS channel and investigate how the device performance is affected upon the addition of the polyelectrolytes and further, how these changes can be translated into an efficient bio-sensing strategy. In particular, we show that the addition of a charged layer can modulate injection of ions into the channel, allowing for sensing applications in physiologically relevant electrolyte concentrations. A similar modulation effect was previously achieved by Magliulo *et al*., via the use of a phospholipid bilayer on top of an organic semiconductor channel of an electrolyte gated field effect transistor. [27] As a proof of concept, we show the use of our LbL modified OECTs for the controlled immobilization as well as electrical detection of nucleic acids, en route to design more sophisticated biosensing systems. Since the technique allows for control over film formation, LbL modified transistors sense nucleic acids with a higher sensitivity and broader dynamic range compared to unmodified devices.

EXPERIMENTAL SECTION

Fabrication of OECTs

The devices are fabricated photolithographically using a parylene-C lift-off process.[28] Patterned gold lines serving as source, drain, and gate electrodes were patterned using Shipley 1813 photoresist, exposed to UV light with a SUSS MJB4 contact aligner, developed in MF-26 followed by thermal evaporation of chromium (10 nm) and gold (100 nm) and metal lift-off in acetone/isopropanol. Two 2 μm thick parylene C layers (SCS Coating) separated by an anti-adhesive (industrial cleaner, Micro-90) were successively deposited using a SCS Labcoater 2. The first parylene layer, was attached to the substrate via an adhesion promoter, namely 3 (trimethoxysilyl)propyl methacrylate (A-174 Silane). For the patterning of the PEDOT:PSS channel (W/L, 100 μm/10 μm), AZ9260 photoresist was spin cast, exposed, and developed in AZ developer (AZ Electronic Materials) followed by reactive ion etching by O_2 plasma (Oxford 80 Plasmalab plus) of the unprotected parts of parylene. The deposition parameters of the PEDOT:PSS films is as follows.

Preparation and biofunctionalization of PEDOT:PSS films with the LbL assemblies

For the deposition of PEDOT:PSS films on transistor channels, a formulation of the commercial aqueous dispersion PH-1000 (Heraeus Clevios GmbH), consisting of 5%V/V ethylene glycol, 0.4%V/V dodecyl benzene sulphonic acid and 25wt% of polyvinyl alcohol was sonicated before spin-casting (2500rpm/ 35sec, for a thickness of 90 nm). The resulting films were subsequently baked at 110 °C for 1 h followed by 2 rinsing/soaking cycles in deionized water to remove any excess of low molecular weight compounds. For the polyelectrolyte assembly, PLL (MW: 70-150 kPa, Sigma Aldrich) and PSS (MW: 70kPa, Sigma Aldrich) at concentrations of 1 mg/ml in PBS were sequentially cast on the unmodified PEDOT:PSS films.

During the PEM construction, each polyelectrolyte was left on top of the film for 20 min and all rinsing steps were performed with an aqueous solution of PBS at pH 7. In the particular case of the covalent attachment of the PLL initial layer, the PEDOT:PSS film was further modified as follows. O_2 plasma treatment (Oxford 80 Plasmalab plus) at mild conditions (25Watt/ 1min) was applied to modify the surfaces with hydroxyl groups for subsequent silanization via a condensation reaction. 3-glycidoxy-propyltrimethoxysilane (GOPS) was deposited by vapor deposition at 90^{o}C for 1h under vacuum. The films were then baked after washing with ethanol (15 sec) for the formation of the epoxy-modified surface. PLL solution at pH 9 was cast on top of these functionalized films and left for 2h. For the fluorescent-based evaluation of the PLL layer on top of PEDOT:PSS, a fluorescein isothiocyanate (FITC) labeled PLL of 1 mg/ml in PBS (MW: 15-30 kDa, Sigma-aldrich) was immobilized on a PEDOT:PSS patterned glass-slide and monitored with a fluorescence microscope (Axio Observer Z1, Carl Zeiss MicroImaging GmbH).

Assessment of LbL assembly on top of PEDOT:PSS films via Quartz Crystal Microbalance with Dissipation module (QCM-D)

The QCM-D measurements were carried out on a commercially available Q-Sense E4 instrument. (LOT-QuantumDesign, France). All measurements were carried out at 25 ℃ with a flow rate of 50 μl/min controlled by a peristaltic pump. PEDOT:PSS films were cast on sensor crystals (SiO_2) as described above. After stabilization in PBS, PLL and PSS were alternately injected into the system for a duration of 20 min for each polyelectrolyte. The sensors were rinsed with PBS after each layer formation. The assembly of PEMs was monitored through changes in resonance frequency (Δf) and energy dissipation (ΔD) of crystals as a function of time

using several overtones. All QCM-D data presented in this paper were measured at the fifth overtone.

Assessment of the film morphology using Atomic Force Microscopy (AFM)

The AFM investigation was carried out using a commercially available (Bruker) instrument. For better image acquisition, tapping mode was used at a scan rate of 1.0-1.2 Hz, with ultrasharp silicon cantilevers at a resolution of 512 points per line.

Characterization of the LbL modified OECTs

All measurements were performed using a Ag/AgCl wire (Warner Instruments) as the gate electrode and PBS or PBS diluted in DI water (pH 7.4), as electrolyte. The steady-state measurements of the OECT (output and transfer curves) were performed using a Keithley 2612A with customized LabVIEW software. For the transient characterization of the OECTs, an NI-PXI-4071 digital multimeter was employed to simultaneously measure drain and gate current (I_D and I_G). For the transient response, a square pulse was applied to the gate and the drain current was measured. The response time of the devices was determined using an exponential fit on the I_D profile. For the frequency dependent measurements, a sinusoidal voltage signal was applied at the gate, with varying frequency and amplitude (ΔV_G=10 mV peak-to-peak, 1 Hz < f< 20 kHz), while measuring I_D (at a constant drain voltage, V_D, of 0.6 V), and therefore transconductance (g_m) as a function of frequency. The recorded signals were saved using customized LabVIEW and analyzed with Matlab.

RNA immobilization on OECTs and its characterization

For the nucleic acid immobilization on the transistor channel, increasing concentrations of single stranded mRNA (0.01 – 50 ng/ml) were deposited on the device and left for 30 min in humid conditions to avoid evaporation. Subsequently, the devices were rinsed in PBS and characterized. The I_D was extracted at a specific operation conditions (V_G= 0V and V_D=-0.6V) and for the different RNA concentrations and a calibration curve of the mRNA immobilization/detection was generated.

RESULTS AND DISCUSSION

LbL on top of PEDOT:PSS : Optimizing the immobilization of the supporting layer by QCM-D

PLL and PSS were chosen in this work as the positively and the negatively charged polyelectrolytes respectively, for alternated deposition on top of PEDOT:PSS. PLL is a polypeptide with pKa values ranging between 9 to 11 due to its amino side groups,[29] while the sulfonic acid groups of PSS result in pKa values ranging from 0.5 to 1.5. [30] Figure 1a shows the chemical structures of all the polymers, along with a schematic representation of the LbL assembly on top of PEDOT:PSS.

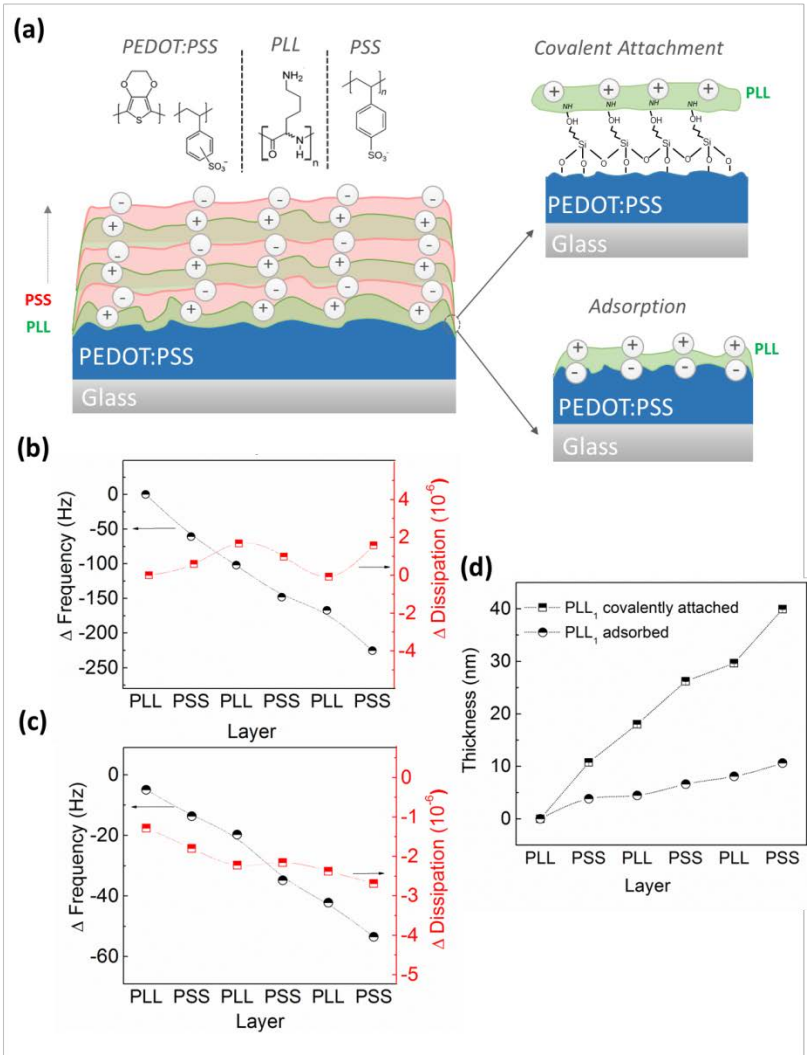

Figure 1. Building an LbL assembly on top of a PEDOT:PSS film. **(a)** Chemical structures of PEDOT:PSS and of the two polyelectrolytes employed, PLL and PSS and schematic of the PEM built up on top of PEDOT:PSS where the initial PLL layer is either covalently attached to the epoxy-modified PEDOT:PSS or electrostatically adsorbed to PEDOT:PSS film. **(b,c)** Changes in QCM-D frequency (black circles) and dissipation (red squares) properties of the PEDOT:PSS film as consecutive layers are formed for the case of covalent attachment of the supporting PLL layer as well as for the case its electrostatic adsorption, respectively. (**d**) The calculated film

thickness using the Sauerbrey model, upon each layer addition for the two distinct cases, adsorption (circles) and covalent attachment (squares).

Bearing in mind the importance of the direct interface of the CP with the first polyelectrolyte layer, our first goal was to optimize the deposition of this initial layer. In our study, we used two approaches to deposit the first PLL layer: either covalently or via electrostatic adsorption. We utilized an epoxy-terminated silane on top of the plasma activated PEDOT:PSS surface as a means for subsequent polypeptide covalent attachment.[31,32] In order to monitor the *in-situ* LbL assembly formation on PEDOT:PSS film involving these two distinct functionalization approaches, we performed QCM-D measurements. QCM-D is a surface-sensitive technique used typically for the mass and viscoelasticity estimation of materials adsorbed on a quartz crystal. Figure 1b presents the shifts in the frequency and dissipation of the PEDOT:PSS coated SiO_2 crystals as each layer is built up, in the case where the supporting layer PLL, is covalently attached. The presence of this layer on top of the PEDOT:PSS film was as well evidenced by fluorescence microscopy using a fluorescent dye-conjugated analog of PLL (PLL-FITC) (Figure S1). During the assembly of the layers, we observe a gradual decrease in frequency and attribute it to the accumulation of polymers on the CP film. Simultaneously, the small change in dissipation ($\Delta D < 1.7 \times 10^{-6}$) reveals the rigidity of the assembled film. The second approach relied on electrostatic adsorption of the initial PLL layer and the associated QCM-D signals summarized in Figure 1c indicate that the LbL formed herein is significantly thinner than for the case of the covalently attached PLL. Moreover, a gradual decrease in the dissipation values with each successive layer indicates that the structure gets softer. The properties of this assembly in terms of thickness and softness are similar to an identical one formed on a bare SiO_2 crystal (Figure S2). Overall, it is likely that the properties of the initial layer, governed by how it is

deposited - either electrostatically or via covalent attachment, affect not only the thickness but also the softness of the final assembly – for at least three consecutive bilayers shown in this study. AFM studies demonstrate no significant morphological differences between these different foundation layers, as well as between the PEMs built on top them (**Figure S3**). The uppermost PSS film was, however, thicker for the case of covalently attached PLL layer. These results are in agreement with several studies reporting on the versatility of the LbL technique. Depending on the targeted application, process parameters can be fine-tuned modulating LbL film properties in return.[33,34] The specific needs of an application would therefore determine the optimum biofunctionalization approach. [32]

Characterization of LbL on top of an OECT

The LbL assembled film was subsequently implemented in a device configuration, and built-up on top of the channel of an OECT, as shown in Figure 2a. We chose to use the approach based on the covalently attached supporting layer, since the resulting film was found to be more rigid through the QCM-D studies and we anticipated that the low potentials applied for the OECT characterization would not affect the assembly. The typical steady-state characteristics of the OECT prior to any surface modification on the channel are shown in Figure S4a. Upon each layer addition, we observe a decrease in the current passing through the channel between the source and drain electrodes (I_D) (Figure 2b). It is plausible that upon contact with the transistor channel, the positively charged PLL de-dopes PEDOT:PSS due to electrostatic interactions with the negatively charged sulfonate groups on the PSS that normally compensate for the mobile holes in PEDOT. This would lower the charge carrier density in the channel and consequently its electrical conductivity. Additional layers on the other hand could contribute to further de-doping.

To elucidate this potential mechanism, we investigated the effect of the layers on the electrical conductance of the channel. For these measurements, the gate electrode was taken out of the electrolyte solution and the I-V characteristics of three identical PEDOT:PSS channels between gold contacts were recorded, upon each layer formation. While the first PLL layer increases the resistance of the channel slightly, the conductance seems to recover as the PSS layer is added (Figure 2c). Nevertheless, we do not observe a clear trend dependent on the polyelectrolyte on top.

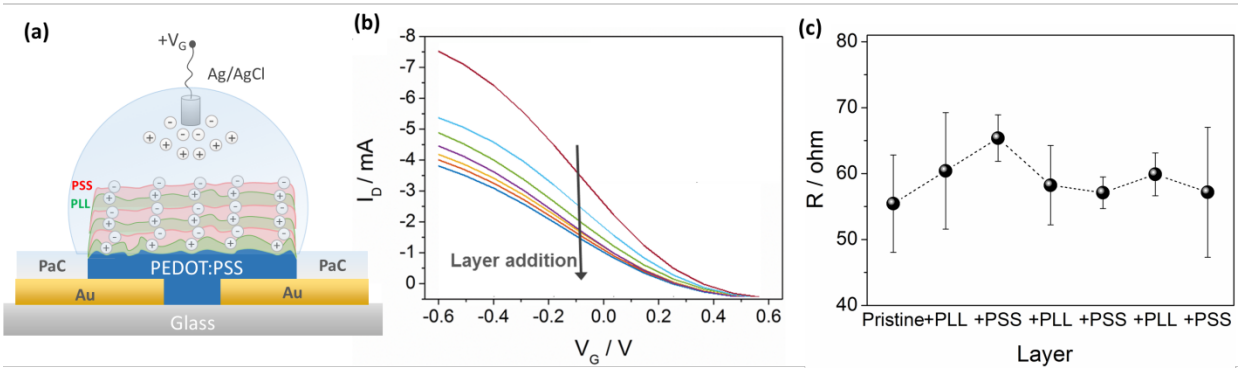

Figure 2. Steady state characteristics of the LbL modified OECT. **(a)** Schematic representation of an LbL modified channel of an OECT. Upon application of a positive gate bias ($+V_G$), cations of the electrolyte are injected into the channel, modulating its conductivity; thereby changing the current between the source and drain contacts (I_D). The gate electrode is Ag/AgCl, parylene (PaC) is the insulator and gold (Au) is used as the contacts of the electrodes. **(b)** Transfer curves recorded at V_D = - 0.6 V after formation of each polyelectrolyte layer. **(c)** The resistance of the channel as a function of consecutive layers deposited. The electrolyte is 0.1 X PBS.

One possible explanation for the decrease in I_D with successive layers is that each polyelectrolyte layer adds an additional capacitance to the ionic circuit between the gate and the channel.[35] OECTs are typically described by an electronic (within the channel) and an ionic

circuit (along the gate and the channel) which may be thought of as a capacitor in series with a resistor.[35] The capacitance term here includes the two electrode/electrolyte interfaces. Since we use a nonpolarizable Ag/AgCl electrode as the gate, the application of V_G induces a steady-state current in the electrolyte endorsed by oxidation/reduction reactions at the gate. The device performance is thus affected by the channel/electrolyte interface where almost all the potential drop takes place.[36] We anticipate that as a new charged layer is formed on top of PEDOT:PSS, the potential profile in the electrolyte is modulated, irrespective of the polarity of pendant groups. In fact, as the polyelectrolytes accumulate on top of PEDOT:PSS, not only does the I_D decrease, but also the gating of the channel becomes less effective, as shown by the gradual decrease in transconductance ($g_m=\Delta I_D/\Delta V_G$) (Figure S4b). This shows that the trend observed in the I-V characteristics that are related to changes in the ionic circuit, is visible due to the inherent amplification of the OECT.

The decrease in the g_m led us to investigate whether the films act as blocking layers and prevent free charges in the electrolyte from entering the channel. This would be best reflected in the temporal response of the device and, in a similar fashion, has been used to evaluate the integrity of barrier forming tissues.[25,26,37] We therefore recorded the transient characteristics of the devices before and after addition of the polyelectrolytes using two techniques which differ by the type of pulses applied at the gate; either sinusoidal or square. In the case of a sinusoidal voltage signal applied with varying frequency and amplitude, the resulting drain current is measured and extracted as the g_m of the OECT as a function of frequency.[39] Typically, below the device cut-off, the ions from the electrolyte can readily enter the channel and the OECT exhibits stable and high g_m. Above the device cut-off, however, the g_m drops since the ions do not have enough time to move into the channel, and this defines the speed of the transistor (see Figure

S5a). Square voltage pulses at the gate similarly modify the drain current and the switching speed of the transistor is then extracted from the obtained current-time profiles.

Figure 3a shows the change in the cut-off frequency upon addition of each polyelectrolyte layer. Rather than a continuous barrier for ions, which would result in a gradual decrease in switching speed, we observe a "ping-pong" effect with the alternating polyelectrolyte layers. For instance, the OECTs switch slower with the initial PLL layer (lower cut-off), but recover their speed (higher cut-off) with the addition of a PSS layer; a trend that is consistent for the consecutive layers. We observe the same trend upon application of a square pulse at the gate electrode (Figure 3b). Moreover, with an increase in the bias magnitude at the gate (V_G=500mV), devices that contain PSS as the uppermost layer recover to the initial switching speed more efficiently.

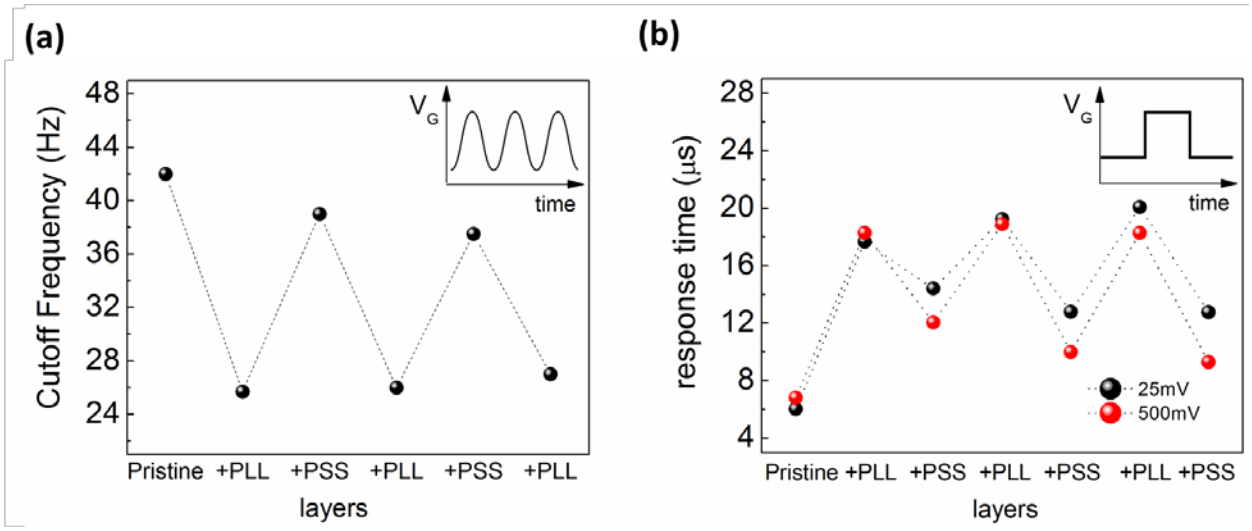

Figure 3. Transient characteristics of the LbL modified OECT. **a**) The change in the cut-off frequency of the devices upon addition of polyelectrolyte layers. The cut-off frequency was estimated from transconductance *vs* frequency plots acquired for each device configuration. **b**) The change in the response time of the devices determined from the drain current response to a

square pulse at the gate which is 25mV (black) and 500 mV (red). All experiments were performed at PBS (diluted 100X).

In a multilayer assembly based on sequential adsorption of oppositely charged polyelectrolytes such as the one used here, once the polyelectrolyte is in excess, the "fixed charges" render the multilayer semi-permeable to ions. The electric potential difference between the PEM surface and the electrolyte is known as the Donnan potential and typically results in the repulsion of mobile ions of the same polarity with the fixed ions at the uppermost polyelectrolyte layer.[40] In our case, based on the transient behavior of the OECT, we observe that the Donnan exclusion effect is taking place when the PLL is the uppermost layer, since it requires more time for the cations to enter and dedope the channel. This leads us to hypothesize that the PSS intrinsically compensates for the PLL beneath and that there is a small excess of charges uncompensated on the PSS surface acting as the driving force for subsequent polyelectrolyte deposition. Due to the reduced repulsion/attraction, when PSS is the outermost layer, ions have less difficulty in entering the film. Furthermore, the increase in the injection bias (gate voltage) helps the ions to interact with PEDOT:PSS. Notably, in contrast to steady-state characteristics, the LbL-induced changes in the transient profile were more pronounced when the measurements were performed at dilute electrolyte concentrations (diluted 100X) as shown in Figure S5b.

LbL for the controlled immobilization and monitoring of nucleic acid

Similar to alternate adsorption of polyelectrolyte systems, LbL can be used to deposit almost any type of charged species, e.g., oligonucleotides: RNA, DNA.[15] In particular, nucleic acid detection using organic electronic devices has received interest in the recent years as a label-free, faster more cost-effective method for diagnostic applications.[41,42] Non-specific RNA sensing has

applications for example in viral diagnostics, when probing the RNA release from a purified virus.[43] As a proof-of-concept for biosensing, we used our LbL functionalized OECTs for electrical monitoring of a nucleic acid. The platform is based on the electrostatic adsorption of a single stranded negatively charged polymer (mRNA; messenger ribonucleic acid), onto the positively charged PLL layer of the LbL immobilized on top of the transistor channel. At physiologically relevant buffer concentration (1 X PBS), mRNA attachment does not lead to any notable change in the transient characteristics of the LbL modified OECT (Figure S5c). On the other hand, we observe a continuous decrease in the steady-state drain current values upon increasing mRNA concentration in the solution (Figure 4a). Note that without the PLL functionalization, PEDOT:PSS devices are insensitive to mRNA, even at a relatively high concentration, indicating that the polymer does not have non-specific interactions with the channel (Figure 4b and S6).

Figure 4b shows the calibration curves of the mRNA loading with respect to the normalized current response of the OECT for a selected gate voltage (V_G=0 V) Here, we compare the detection sensitivity of two devices, one comprising an LbL modified channel, and a second which contains only one layer of PLL. We note that the response observed upon binding of mRNA is predominantly linear, although at lower concentrations, there may be some cooperativity type effects.[44] The mechanism of detection is based on the compensation of charges on the backbone of the mRNA, by positive charges on the upper layer of PLL. However, there may be more complex interactions occurring between the polypeptide and the nucleotide such as hydrogen bonding and hydrophobic interactions,[45] which will merit further investigation. There appears to be a difference in sensing capability of one versus the other: we posit that in the case of an LbL modified surface there is likely a more even surface charge distribution on the

uppermost layer of the LbL which may enable sensing with a broader dynamic range and higher sensitivity. In other words, the effect observed upon binding of mRNA to the LbL modified OECT appears not to saturate as early as that seen on a PLL modified device. Notably, the measurement error is larger for the OECT comprising a single PLL layer as the sensing-active component compared to the device modified with the LbL assembly.

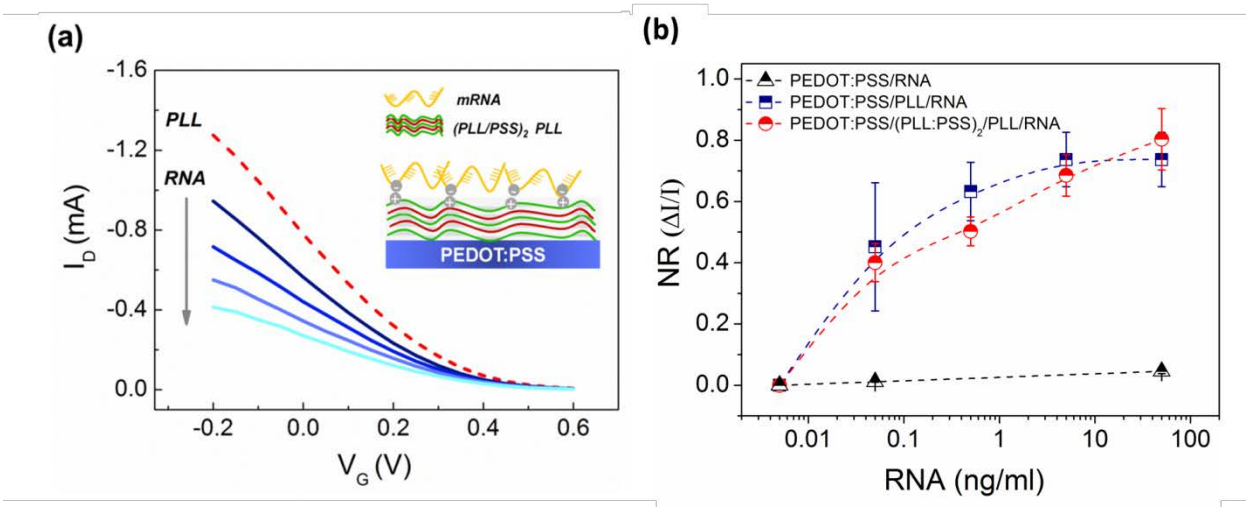

Figure 4. RNA sensing using LbL modified OECT. **a**) The change in transfer characteristics of the LbL modified OECT upon additions of increasing concentrations of the mRNA **b**) Comparative mRNA titration curves at V_G = 0 V for an LbL modified device, a single layer PLL modified device and for a typical device (i.e. bare PEDOT:PSS in the channel serving as the control), showing an increased sensitivity with a broader linear range for the LbL assembly. All experiments were performed at physiologically relevant concentrations. The error bars were deduced from four measurements on two identical channels (100*10 µm in length*width).

The drawback of most electrolyte gated transistors used for sensing of such electrically charged species is the necessity to use low salt concentrations due to the Debye length limitations. [46,47] Current-voltage characteristics of LbL modified OECTs are, on the other hand, sensitive to RNA at ionic concentrations similar to those found in biological media such as the blood. Similar to the effect of the charged layers on top of the OECT, acting as an additional capacitor to our circuit, RNA layer changes the potential profile at the electrolyte shown at the steady state measurements.

CONCLUSIONS

In conclusion, we functionalized the conducting polymer channel of OECTs with an LbL assembly of polyelectrolytes, aiming to confer new functionalities on the device. This highly versatile technique enables fine tuning of crucial film parameters such as thickness and rigidity. We find that the PEMs modulate the electrical potential in the electrolyte and affect the injection of ions into the channel, which we utilize as a strategy to sense charged biological species such as mRNA. The LbL modified OECTs are able to sense nucleic acid in the electrolyte with a high sensitivity and broad linear range at low operating voltages. Notably, the devices signal the presence of mRNA at physiologically relevant electrolyte concentrations, visible in the steady state current profile. Future experiments will address specific nucleic acid detection using a complementary probe based on our LbL functionalization method.

ACKNOWLEDGMENTS

A-M. P and S. I. contributed equally to the present work. This work was supported by the Marie Curie ITN project OrgBio No. 607896 and the Agence Nationale de la Recherche 3Bs

project. The authors are grateful to Alberto Salleo for fruitful discussions, and to NeuroSys for the kind gift of mRNA.

AUTHOR INFORMATION

Corresponding Authors: owens@emse.fr; sahika.inal@kaust.edu.sa. Anna-Maria Pappa and Sahika Inal contributed equally to this work.

ASSOCIATED CONTENT

Supporting information: Transfer characteristics of a pristine OECT and after addition of mRNA; The transconductance (g_m) vs. frequency plots of an OECT channel upon each consecutive polyelectrolyte formation; Typical output characteristics of the OECT prior to any surface modification on top of the channel; Changes in QCM-D frequency and dissipation of a SiO_2 crystal upon formation of an LbL assembly of PEMs; Fluorescence microscopy image of the fluorescein isothiocyanate (FITC) labeled PLL covalently attached on the surface of epoxy-modified PEDOT:PSS and AFM images of the LbL modified PEDOT:PSS films.

REFERENCES

(1) Chiang, C. K.; Fincher, C. R.; Park, Y. W.; Heeger, A. J.; Shirakawa, H.; Louis, E. J.; Gau, S. C.; MacDiarmid, A. G. Electrical Conductivity in Doped Polyacetylene. *Phys. Rev. Lett.* **1978**, *40* (22), 1472–1472.

(2) Simon, D. T.; Gabrielsson, E. O.; Tybrandt, K.; Berggren, M. Organic Bioelectronics: Bridging the Signaling Gap between Biology and Technology. *Chem. Rev.* **2016**, *116* (21), 13009–13041.

(3) Guimard, N. K.; Gomez, N.; Schmidt, C. E. Conducting Polymers in Biomedical Engineering. *Prog. Polym. Sci.* **2007**, *32*, 876–921.

(4) Owens, R. M.; Malliaras, G. G. Organic Electronics at the Interface with Biology. *MRS Bull.* **2011**, *35* (06), 449–456.

(5) Molino, P. J.; Yue, Z.; Zhang, B.; Tibbens, A.; Liu, X.; Kapsa, R. M. I.; Higgins, M. J.; Wallace, G. G. Influence of Biodopants on PEDOT Biomaterial Polymers: Using QCM-D to Characterize Polymer Interactions with Proteins and Living Cells. *Adv. Mater. Interfaces* **2014**, *1* (3), 1300122.

(6) Goddard, J. M.; Hotchkiss, J. H. Polymer Surface Modification for the Attachment of Bioactive Compounds. *Prog. Polym. Sci.* **2007**, *32* (7), 698–725.

(7) Inal, S.; Rivnay, J.; Hofmann, A. I.; Uguz, I.; Mumtaz, M.; Katsigiannopoulos, D.; Brochon, C.; Cloutet, E.; Hadziioannou, G.; Malliaras, G. G. Organic Electrochemical Transistors Based on PEDOT with Different Anionic Polyelectrolyte Dopants. *J. Polym. Sci. Part B Polym. Phys.* **2016**, *54* (2), 147–151.

(8) *Iontronics: Ionic Carriers in Organic Electronic Materials and Devices*; Leger, J., Berggren, M., Carter, S., Eds.; CRC Press: Boca Raton, FL, 2010**.**

(9) Decher, G.; Hong, J. D.; Schmitt, J. Buildup of Ultrathin Multilayer Films by a Self-Assembly Process: III. Consecutively Alternating Adsorption of Anionic and Cationic Polyelectrolytes on Charged Surfaces. *Thin Solid Films* **1992**, *210–211*, 831–835.

(10) Ariga, K.; Hill, J. P.; Ji, Q. Layer-by-Layer Assembly as a Versatile Bottom-up Nanofabrication Technique for Exploratory Research and Realistic Application. *Phys. Chem. Chem. Phys.* **2007**, *9* (19), 2319–2340.

(11) Rydzek, G.; Ji, Q.; Li, M.; Schaaf, P.; Hill, J. P.; Boulmedais, F.; Ariga, K. Electrochemical Nanoarchitectonics and Layer-by-Layer Assembly: From Basics to Future. *Nano Today* **2015**, *10* (2), 138–167.

(12) Vendra, V. K.; Wu, L.; Krishnan, S. *Polymer Thin Films for Biomedical Applications*; Nanomaterials for the Life Sciences 5; Wiley-VCH:Weinheim, Germany, 2010, pp 1–54.

(13) Pérez, R. A.; Won, J. E.; Knowles, J. C.; Kim, H. W. Naturally and Synthetic Smart Composite Biomaterials for Tissue Regeneration. *Adv. Drug Deliv. Rev.* **2013**, *65* (4), 471–496.

(14) Boudou, T.; Crouzier, T.; Ren, K.; Blin, G.; Picart, C. Multiple Functionalities of Polyelectrolyte Multilayer Films: New Biomedical Applications. *Adv. Mater.* **2009**, *22* (4), 441–467.

(15) Diéguez, L.; Darwish, N.; Graf, N.; Vörös, J.; Zambelli, T. Electrochemical Tuning of the Stability of PLL/DNA Multilayers. *Soft Matter* **2009**, *5* (12), 2415–2421.

(16) Wohl, B. M.; Engbersen, J. F. J. Responsive Layer-by-Layer Materials for Drug Delivery. *J. Control. Release* **2012**, *158* (1), 2–14.

(17) Wood, K. C.; Zacharia, N. S.; Schmidt, D. J.; Wrightman, S. N.; Andaya, B. J.; Hammond, P. T. Electroactive Controlled Release Thin Films. *Proc. Natl. Acad. Sci. U. S. A.* **2008**, *105* (7), 2280–2285.

(18) Wang, B.; Rusling, J. F. Voltammetric Sensor for Chemical Toxicity Using [Ru(bpy)2poly(4-vinylpyridine)10Cl)]+ as Catalyst in Ultrathin Films. DNA Damage from Methylating Agents and an Enzyme-Generated Epoxide. *Anal. Chem.* **2003**, *75* (16), 4229–4235.

(19) Xu, J.-J.; Zhao, W.; Luo, X.-L.; Chen, H.-Y. A Sensitive Biosensor for Lactate Based on Layer-by-Layer Assembling MnO2 Nanoparticles and Lactate Oxidase on Ion-Sensitive Field-Effect Transistors. *Chem. Commun*. **2005**, (6), 792–794.

(20) Inal, S.; Rivnay, J.; Leleux, P.; Ferro, M.; Ramuz, M.; Brendel, J. C.; Schmidt, M. M.; Thelakkat, M.; Malliaras, G. G. A High Transconductance Accumulation Mode Electrochemical Transistor. *Adv. Mater.* **2014**, *26* (44), 7450–7455.

(21) Khodagholy, D.; Rivnay, J.; Sessolo, M.; Gurfinkel, M.; Leleux, P.; Jimison, L. H.; Stavrinidou, E.; Herve, T.; Sanaur, S.; Owens, R. M.; Malliaras, G. G. High Transconductance Organic Electrochemical Transistors. *Nat. Commun.* **2013**, *4*, 2133.

(22) Sessolo, M.; Rivnay, J.; Bandiello, E.; Malliaras, G. G.; Bolink, H. J. Ion-Selective Organic Electrochemical Transistors. *Adv. Mater.* **2014**, *26* (28), 4803–4807.

(23) Tang, H.; Yan, F.; Lin, P.; Xu, J.; Chan, H. L. W. Highly Sensitive Glucose Biosensors Based on Organic Electrochemical Transistors Using Platinum Gate Electrodes Modified with Enzyme and Nanomaterials. *Adv. Funct. Mater.* **2011**, *21* (12), 2264–2272.

(24) Pappa, A.-M.; Curto, V. F.; Braendlein, M.; Strakosas, X.; Donahue, M. J.; Fiocchi, M.; Malliaras, G. G.; Owens, R. M. Organic Transistor Arrays Integrated with Finger-Powered Microfluidics for Multianalyte Saliva Testing. *Adv. Healthc. Mater.* **2016**, *5* (17), 2295–2302.

(25) Ramuz, M.; Hama, A.; Rivnay, J.; Leleux, P.; Owens, R. Monitoring of Cell Layer Coverage and Differentiation with the Organic Electrochemical Transistor. *J. Mater. Chem. B* **2015**, *3* (29), 5971–5977.

(26) Tria, S. A.; Ramuz, M.; Jimison, L. H.; Hama, A.; Owens, R. M. Sensing of Barrier Tissue Disruption with an Organic Electrochemical Transistor. *J. Vis. Exp.* **2014**, No. 84, e51102.

(27) Magliulo, M.; Mallardi, A.; Mulla, M. Y.; Cotrone, S.; Pistillo, B. R.; Favia, P.; Vikholm-Lundin, I.; Palazzo, G.; Torsi, L. Electrolyte-Gated Organic Field-Effect Transistor Sensors Based on Supported Biotinylated Phospholipid Bilayer. *Adv. Mater.* **2013**, *25* (14), 2090–2094.

(28) Sessolo, M.; Khodagholy, D.; Rivnay, J.; Maddalena, F.; Gleyzes, M.; Steidl, E.; Buisson, B.; Malliaras, G. G. Easy-to-Fabricate Conducting Polymer Microelectrode Arrays. *Adv. Mater.* **2013**, *25* (15), 2135–2139.

(29) Choi, J.-H.; Kim, S.-O.; Linardy, E.; Dreaden, E. C.; Zhdanov, V. P.; Hammond, P. T.; Cho, N.-J. Influence of pH and Surface Chemistry on Poly(L -Lysine) Adsorption onto Solid Supports Investigated by Quartz Crystal Microbalance with Dissipation Monitoring. *J. Phys. Chem. B* **2015**, *119* (33), 10554–10565.

(30) Lewis, S. R.; Datta, S.; Gui, M.; Coker, E. L.; Huggins, F. E.; Daunert, S.; Bachas, L.; Bhattacharyya, D. Reactive Nanostructured Membranes for Water Purification. *Proc. Natl. Acad. Sci. U. S. A.* **2011**, *108* (21), 8577–8582.

(31) Strakosas, X.; Sessolo, M.; Hama, A.; Rivnay, J.; Stavrinidou, E.; Malliaras, G. G.; Owens, R. M. A Facile Biofunctionalisation Route for Solution Processable Conducting Polymer Devices. *J. Mater. Chem. B* **2014**, *2* (17), 2537–2545.

(32) Strakosas, X.; Wei, B.; Martin, D. C.; Owens, R. M. Biofunctionalization of Polydioxythiophene Derivatives for Biomedical Applications. *J. Mater. Chem. B* **2016**, *4* (29), 4952–4968.

(33) El Haitami, A. E.; Martel, D.; Ball, V.; Nguyen, H. C.; Gonthier, E.; Labbé, P.; Voegel, J.-C.; Schaaf, P.; Senger, B.; Boulmedais, F. Effect of the Supporting Electrolyte Anion on the Thickness of PSS/PAH Multilayer Films and on Their Permeability to an Electroactive Probe. *Langmuir* **2009**, *25* (4), 2282–2289.

(34) Kolasińska, M.; Krastev, R.; Warszyński, P. Characteristics of Polyelectrolyte Multilayers: Effect of PEI Anchoring Layer and Posttreatment after Deposition. *J. Colloid Interface Sci.* **2007**, *305* (1), 46–56.

(35) Bernards, D. A.; Malliaras, G. G. Steady-State and Transient Behavior of Organic Electrochemical Transistors. *Adv. Funct. Mater.* **2007**, *17* (17), 3538–3544.

(36) Demelas, M.; Scavetta, E.; Basiricò, L.; Rogani, R.; Bonfiglio, A. A Deeper Insight into the Operation Regime of All-Polymeric Electrochemical Transistors. *Appl. Phys. Lett.* **2013**, *102* (19), 193301.

(37) Tria, S. A.; Jimison, L. H.; Hama, A.; Bongo, M.; Owens, R. M. Validation of the Organic Electrochemical Transistor for in Vitro Toxicology. *Biochim. Biophys. Acta* **2013**, *1830* (9), 4381–4390.

(38) Ramuz, M.; Hama, A.; Rivnay, J.; Leleux, P.; Owens, R. M. Monitoring of Cell Layer Coverage and Differentiation with the Organic Electrochemical Transistor. *J Mater Chem B* **2015**, *3* (29), 5971–5977.

(39) Rivnay, J.; Ramuz, M.; Leleux, P.; Hama, A.; Huerta, M.; Owens, R. M. Organic Electrochemical Transistors for Cell-Based Impedance Sensing. *Appl. Phys. Lett.* **2015**, *106* (4), 043301.

(40) Calvo, E. J.; Wolosiuk, A. Donnan Permselectivity in Layer-by-Layer Self-Assembled Redox Polyelectrolye Thin Films. *J. Am. Chem. Soc.* **2002**, *124* (28), 8490–8497.

(41) Lai, S.; Demelas, M.; Casula, G.; Cosseddu, P.; Barbaro, M.; Bonfiglio, A. Ultralow Voltage, OTFT-Based Sensor for Label-Free DNA Detection. *Adv. Mater.* **2013**, *25* (1), 103–107.

(42) Demelas, M.; Lai, S.; Casula, G.; Scavetta, E.; Barbaro, M.; Bonfiglio, A. An Organic, Charge-Modulated Field Effect Transistor for DNA Detection. *Sens. Actuators, B* **2012**, *171*, 198–203.

(43) Hsu, H.-L.; Millet, J. K.; Costello, D. A.; Whittaker, G. R.; Daniel, S. Viral Fusion Efficacy of Specific H3N2 Influenza Virus Reassortant Combinations at Single-Particle Level. *Sci. Rep.* **2016**, *6*, 35537.

(44) Liu, G.; Molas, M.; Grossmann, G. A.; Pasumarthy, M.; Perales, J. C.; Cooper, M. J.; Hanson, R. W. Biological Properties of Poly-L-Lysine-DNA Complexes Generated by Cooperative Binding of the Polycation. *J. Biol. Chem.* **2001**, *276* (37), 34379–34387.

(45) Jones, S.; van Heyningen, P.; Berman, H. M.; Thornton, J. M. Protein-DNA Interactions: A Structural Analysis. *J. Mol. Biol.* **1999**, *287* (5), 877–896.

(46) Kergoat, L.; Piro, B.; Berggren, M.; Pham, M.-C.; Yassar, A.; Horowitz, G. DNA Detection with a Water-Gated Organic Field-Effect Transistor. *Org. Electron.* **2012**, *13* (1), 1–6.

(47) Wang, D.; Noël, V.; Piro, B. Electrolytic Gated Organic Field-Effect Transistors for Application in Biosensors - A Review. *Electronics* **2016**, *5* (1), 9.

Table of Contents: